UDK 669.715:621.762:621.762.5
Original scientific article/Izvirni znanstveni članek

ISSN 1580-2949
MTAEC9, 49(1)129(2015)

COMPACTING THE POWDER OF Al-Cr-Mn ALLOY WITH SPS

KOMPAKTIRANJE PRAHU ZLITINE Al-Cr-Mn S SPS

Tomáš František Kubatík[1], Zdeněk Pala[1], Pavel Novák[2]

[1]Institute of Plasma Physics AS CR, Za Slovankou 1782/3, 182 00 Prague 8, Czech Republic
[2]Department of Metals and Corrosion Engineering, Institute of Chemical Technology, Technická 5, 166 28 Prague 6, Czech Republic
kubatik@ipp.cas.cz

Prejem rokopisa – received: 2014-02-11; sprejem za objavo – accepted for publication: 2014-02-26

Rapidly solidified powder AlCr6Fe2(Mn, Si, Ti) obtained with the melt atomization contained a solid solution of the alloying elements in aluminium and $Al_{57}Mn_{12}$, $Al_{42}Cr_7$(Fe) and Al_2Cr_3(Fe) intermetallic phases. The addition of chromium to aluminium alloys is acknowledged to efficiently inhibit the growth of refined Al grains. Spark-plasma sintering (SPS) is a modern method where the diffusion and decomposition of metastable intermetallics are limited due to the high speed of the process and lower sintering temperatures. This work investigates a compaction of Al-Cr-Fe-Si alloy powders using this method.

Keywords: aluminium alloy, intermetallics, powder metalurgy, spark-plasma sintering

Hitro strjen prah AlCr6Fe2(Mn, Si, Ti), dobljen z atomizacijo taline, je vseboval trdno raztopino legirnih elementov v aluminiju in intermetalne faze $Al_{57}Mn_{12}$, $Al_{42}Cr_7$(Fe), Al_2Cr_3(Fe). Dodatek kroma aluminiju učinkovito zadržuje rast drobnih zrn Al. Sintranje z iskrasto plazmo (SPS) je sodobna metoda, kjer je omejena difuzija in razgradnja metastabilnih intermetalnih zlitin zaradi velike hitrosti procesa in nižjih temperatur sintranja. V tem delu se raziskuje kompaktiranje prahov zlitine Al-Cr-Fe-Si po metodi SPS.

Ključne besede: aluminijeva zlitina, intermetalne faze, prašna metalurgija, sintranje z iskrasto plazmo

1 INTRODUCTION

Aluminium alloys with transition metals (e.g., Fe, Cr) have been known as attractive materials with an excellent combination of the tensile strength and thermal stability,[1] which makes them useful for the applications at elevated temperatures in the automotive and aerospace industries.[1] Their thermal stability is attributed to both the fact that these alloying elements have a low diffusion coefficient and their solubility in aluminium. However, these features make these alloys difficult to prepare using conventional metallurgy with a large amount of alloying elements. Therefore, these materials are made with powder metallurgy (PM) using rapidly solidified powders. A general feature of rapidly solidified Al-Cr and Al-Mn based alloys is the presence of many intermetallic phases, including quasi crystals (Q-phases),[2,3] in the intensively cooled alloys.

In the literature, the presence of multiple species of icosahedral quasicrystal phases $Al_{95}Fe_4Cr$ (Ti, Si), $Al_{84.6}Cr_{15.4}$(Ti, Si) and $Al_{74}Cr_{20}Si_6$(Fe, Ti) was described. The authors stated that in a powder fraction of 25–45 μm, phases $Al_{13}Cr_2$, $Al_{82}Fe_{18}$, $Al_{95}Fe_4Cr$ and $Al_{74}Cr_{20}Si_6$ were present, while in a fraction of 100–125 μm only phases $Al_{13}Cr_2$, $Al_{32}Fe_4$ and $Al_{82}Fe_{18}$ were found.[4–6] A quasi-crystalline phase is decomposed at the temperatures around 550 °C.[4,5] It was reported[6] that the compact samples prepared with the methods of cold extrusion, ultra-high pressure (6 GPa) and hot extrusion (480 °C/30 min preheating) had almost no porosity.

The recently developed field-assisted sintering (FAST),[7,8] also known as spark-plasma sintering (SPS),[9–11] or pulsed-electric-current sintering (PECS),[12,13] is a non-conventional powder-consolidation technique used for a very fast densification of ceramic and metal powders. In this method, a powder is placed inside a tool between two pressing punches acting also as electrodes. High-amperage electric-current pulses are passed through the uniaxially pressed powder compact loaded in the tool. The powder is rapidly densified due to a simultaneous application of pressure and heat in accordance with the Joule effect, whereas the grain coarsening is suppressed and the diffusion and decomposition of metastable intermetallics are limited due to the high speed of the process and lower sintering temperatures. The purpose of the present work is to study the compacting of an aluminium-alloy powder using SPS, monitor the changes taking place during the compacting of rapidly solidified powders and compare the structure and phase composition of the obtained samples with the conventional method of hot extrusion.

2 EXPERIMENTAL WORK

The feedstock material for SPS was an atomized (N_2) powder with a composition of AlCr6Fe2(Mn, Si, Ti). The powder was sieved into size fractions of ≤ 32 μm and 160–80 μm. The compacting was carried out in a spark-plasma sintering (SPS) system – model SPS 10-4 (Thermal Technology, USA). The tool system placed inside the vacuum chamber consisted of a graphite punch-and-die unit. The powder was manually poured into the die cavity. The temperature was measured with a NiCr-Ni thermocouple.

Figure 1 is a standard record of a single cycle. The program begins with the evacuation of the chamber. Afterwards, the sample is pre-loaded at 20 MPa, followed by heating with the speed of 100 °C/min, using a pulsed DC source. After reaching the desired process temperature (450, 500 and 550) °C, the sample is loaded to the final compression pressure of 80 MPa. The dwell time at this temperature and pressure is 5 min, as shown in **Figure 1**.

After the dwell time, the DC pulse source is turned off and the sample is cooled down to room temperature with free cooling. After the aeration of the chamber, the graphite tool is opened and the sample is removed. The prepared samples are cylindrical with a diameter of 19 mm and height of 4–6 mm. The porosity of the samples was measured with the Archimedes method. The microstructure was observed in the metallographic cut using a scanning electron microscope EVO MA 15 (Carl Zeiss SMT, Germany, SEM). Both the starting powders, i.e., with the particle sizes smaller than 32 μm and within the range from 160 μm to 180 μm, and the obtained spark-plasma-sintered samples were subjected to X-ray diffraction (XRD) analyses.

The powders were inserted into standard sample holders with the so-called side-loading procedure that minimizes the rise of the preferred orientation. These two samples were measured in the standard Bragg-Brentano geometry with a divergent beam and with a beam knife placed above the samples in order to minimize the effects of air scattering. Since our aim was to further measure the centres of the sintered samples, the irradiated volumes were in the middle of the samples' cross-sections. Therefore, a poly-capillary system and a collimator of 1 mm in diameter were inserted into the primary X-ray beam path changing the originally divergent character into a quasi-parallel one; diffraction CuK_α radiation was detected with a 1D LynxEye detector. The used D8 Discover diffractometer was equipped with a laser system and a compact *x, y, z* stage facilitating precise positioning of the measured surface.

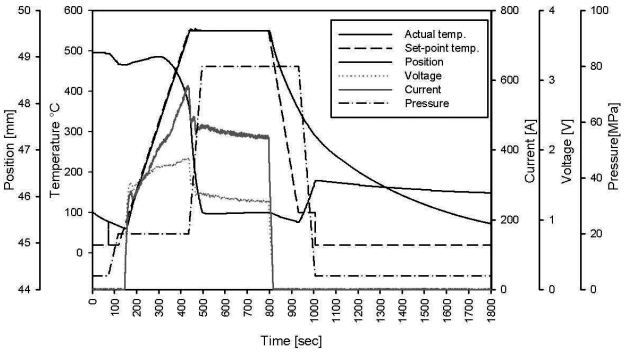

Figure 1: Parameter progress during the sintering of aluminium alloy powder (160–180 μm fraction) at 550 °C (SPS)

Slika 1: Spreminjanje parametrov med sintranjem prahu aluminijeve zlitine (zrnatost 160–180 μm) pri 550 °C (SPS)

3 RESULTS AND DISCUSSION

3.1 Densification behaviour

The diagram in **Figure 1** shows the process parameters during the SPS process at 550 °C for the coarse fraction (160–180 μm). The plots for all the temperatures and fractions are very similar differing only at low temperatures, where a small change in the position can be seen even during the dwell time. The curve of the position, which shows a change in the position of the pistons, indicates that the increasing temperature slightly increases the value of the positions related to thermal heating and auxiliary piston-guide graphite parts. At the temperatures slightly above 300 °C, the softening and deformation of the alloy powder occur (sintering). This temperature is the same for any sintering temperature (450, 500 and 550) °C and powder fraction (32 μm and 160–180 μm).

After reaching the temperature, the pressure increases for one minute, reaching the resulting value of 80 MPa. During the pressure increase, a very sharp reduction in the value of the position is detected, indicating an intensive compaction. After reaching the final pressure, the current values of the temperature and pressure are maintained constant for the duration of 5 min. The sintering temperature of 450 °C leads to a gradual compaction, during the dwell time, of the fraction of the powder smaller than 32 μm but to a smaller extent than for the coarse fraction. This may be related to the fact that the spherical powder alloy has a hard thin oxide layer, whose proportion is smaller in the coarse fraction of the aluminium alloy. This hypothesis is confirmed with the results of the open-porosity measurements, whose values are listed in **Table 1**. The results also show that the sintering temperature of 550 °C results in a very low open porosity, which is almost at the limit of the quantification obtained with the Archimedes method.

Table 1: Open porosity depending on the sintering temperature and powder size

Tabela 1: Odprta poroznost je odvisna od temperature sintranja in od velikosti zrn prahu

	Powder fraction (μm)	Temperature of sintering (°C)	Open porosity (%)
Aluminium alloy	32	450	3.05
Aluminium alloy	32	500	2.63
Aluminium alloy	32	550	0.14
Aluminium alloy	160–180	450	2.88
Aluminium alloy	160–180	500	2.88
Aluminium alloy	160–180	550	0.068

3.2 Microstructure

Figure 2 is a cross-sectional microstructure of the sintered powder fraction of 160–180 μm at 550 °C. The figure shows that the sintered alloy does not contain any visible pores and has a nearly homogeneous structure. In

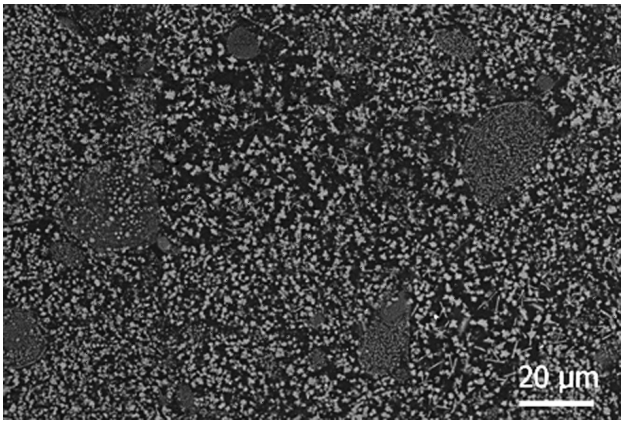

Figure 2: Microstructure of the alloy sintered at 550 °C for 5 min (fraction of 160–180 µm, SEM)

Slika 2: SEM-posnetek mikrostrukture zlitine, sintrane 5 min na 550 °C (zrnatost 160–180 µm)

the microstructure, only some spherical particles can be seen. The structure consists of an aluminium matrix with a small amount of silicon (titanium) in the solid solution, in which $Al_{45}Cr_7$ intermetallic phases consisting of rounded particles with an irregular shape are clearly visible. The observed microstructures are fairly similar at all the compacting temperatures and for both powder fractions.

3.3 XRD – phase analysis

The obtained diffraction patterns are juxtaposed in **Figure 3**. The phase identification revealed, apart from the expected fcc (Fm3m) aluminium solid solution, also aluminium manganese (cubic Pm-3 $Al_{57}Mn_{12}$) and aluminium chromium (monoclinic C12/m1 $Al_{45}Cr_7$) phases. It is clearly seen that the differences between all the SPS-sample diffraction patterns are virtually non-existent and that the peak positions match those of the coarser powder. However, several differences between the diffraction patterns of both powders can be observed

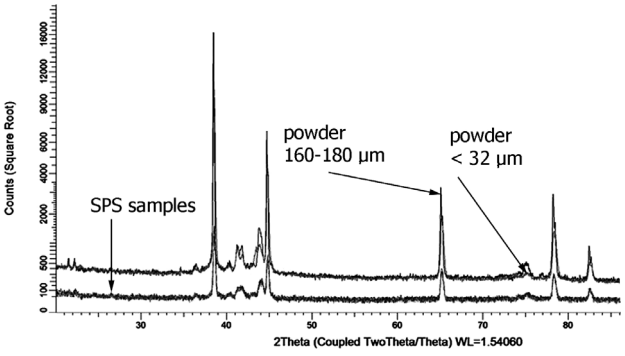

Figure 3: Plain comparison of the obtained diffraction patterns. The substantial difference between the intensities is due to the differences in the irradiated volume of the powders and the centres of the SPS sample cross-sections.

Slika 3: Primerjava dobljenih difrakcijskih vzorcev. Občutna razlika v intenzitetah je zaradi razlik v obsevanem volumnu prahov in sredine prereza SPS-vzorcev.

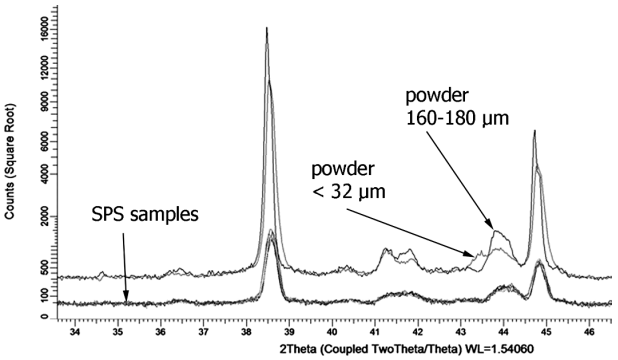

Figure 4: Differences between diffraction-peak positions for the two fractions of the used powder

Slika 4: Razlika med pozicijo difrakcijskih vrhov za dve frakciji uporabljenih prahov

(**Figure 4**) and, hence, the sieving led to minor changes in the phase composition.

The phase ID of the powder with smaller particles gave hints that the Al-Cr-Mn phase could be present. There are only two such phases in the ICSD database, namely, cubic Im-3 $Al_{12}Cr_{0.5}Mn_{0.5}$ and tetragonal I4/mmm Al_2Cr_3Mn. The latter proved to be the one present according to the Rietveld refinement, which gave the quantity of almost w = 1 % of this tetragonal phase. The results of the quantitative Rietveld refinement of both powders are summarized in **Table 2**. Since the diffraction patterns of the sintered samples do not exhibit significant differences, similar information about the phase presence is not relevant and, thus, not provided. Both the Al-Cr (ICSD code of 57652) and Al-Mn (ICSD code of 14374) phases were used for the Rietveld refinement performed in TOPAS 4.2 with sufficiently good matches between the structure model and measured data. There is, however, about the mass fraction 3 % more of the Al-Cr phase in the sintered samples due to various reasons; the difference in the irradiated volume can be one of them.

Table 2: Results of a quantitative Rietveld refinement of both powders

Tabela 2: Rezultati kvantitativnega Rietveldovega udrobljenja obeh prahov

Powder particle fraction	w(Al) /%	w($Al_{57}Mn_{12}$) /%	w($Al_{42}Cr_7$) /%	w(Al_2Cr_3Mn) /%
< 32 µm	63.9	19.0	16.3	0.8
160–180 µm	68.0	9.4	22.6	

mass fraction, w/%

4 CONCLUSIONS

Using the SPS method, a compact alloy with a very low open porosity was prepared. The porosity values are dependent on the powder fraction and sintering temperature. The microstructure of the compacted samples is formed using an aluminium-based solid solution with homogeneously dispersed intermetallic particles $Al_{45}Cr_7$ at all the sintering temperatures. The performed eva-

luation of diffraction data indicates that all the sintered samples are very similar with respect to the phase composition. Moreover, the shapes of diffraction profiles are also the same which means that the real structures, namely, the microstrains and coherent domain sizes, remain virtually the same for all the investigated samples.

It should be noted that the irradiated volumes were in the centre of the cross-sections and, hence, certain differences could occur on the sample surfaces. Nevertheless, we unfolded comparatively significant differences between the phase compositions of both powder fractions. The powder with smaller particles includes almost mass fractions 1 % of the tetragonal Al-Cr-Mn phase, 10 % more of the Al-Mn phase and about 6 % less of the Al-Cr phase. The probable reason for the differences lies in the fact that the powder fractions differ in the cooling rate. Finer powders solidify more rapidly than the coarser ones. This difference can cause changes to the types of intermetallics that are formed. Moreover, the identified phase compositions include more manganese than expected on the basis of the initial chemical composition of the atomized powder. This discrepancy can be explained with, e.g., the substitution of manganese atoms by iron.

The SPS method is a very effective method for compacting alumina-based powders. The sample size is limited by the size of the die. In this case, the whole sample body is heated in accordance with the Joule effect, which enables a production of the samples with almost no porosity at very short dwell times, unlike in the case of hot extrusion. The results of the XRD analysis show that there are almost no observable changes during the SPS compacting process with respect to the phase composition and real structure.

5 REFERENCES

[1] M. J. F. Gándara, Aluminium: the metal of choice, Mater. Tehnol., 47 (**2013**) 3, 261–265

[2] M. Yamasaki, Y. Nagaishi, Y. Kawamure, Inhibition of Al grain coarsening by quasicrystalline icosahedral phase in the rapidly solidified powder metallurgy Al-Fe-Cr-Ti alloy, Scripta Materialia, 56 (**2007**), 785–788

[3] G. Lojen, T. Bončina, F. Zupanič, Thermal stability of Al-Mn-Be Melt-spun ribbons, Mater. Tehnol., 46 (**2012**) 4, 329–333

[4] B. Bártová, D. Vojtěch, J. Verner, A. Gemperle, V. Studnička, Structure and properties of rapidly solidified Al-Cr-Fe-Ti-Si powder alloys, Journal of Alloys and Compounds, 387 (**2005**), 193–200

[5] D. Vojtěch, A. Michalcová, J. Pilch, P. Šittner, J. Šerák, P. Novák, Structure and thermal stability of Al-5.7Cr-2.5Fe-1.3Ti alloy produced by powder metallurgy, Journal of Alloys and Compounds, 475 (**2009**), 151–156

[6] D. Vojtěch, A. Michalcová, F. Průša, K. Dám, P. Šedá, Properties of the thermally stable Al95Cr3.1Fe0.8 alloy prepared by cold-compression at ultra-high pressure and by hot-extrusion, Materials characterization, 66 (**2012**), 83–92

[7] Y. Minamino, Y. Koizumi, M. Tsuji, N. Hirohata, K. Mizuuchi, Y. Ohkanda, Microstructures and mechanical properties of bulk nanocrystalline Fe-Al-C alloys made by mechanical alloying with subsequent spark plasma sintering, Science and Technology of Advanced Materials, 5 (**2004**), 133–143

[8] T. Masao, Handbook of Advanced Ceramics, Chapter 11.2.3 – Spark Plasma Sintering (SPS) Method, System and Applications, Second Edition, 2013, 1149–1177

[9] T. Skiba, P. Haušild, M. Karlík, K. Vanmeensel, J. T. Vleugels, Mechanical properties of spark plasma sintered FeAl intermetallics, Intermetallics, 18 (**2010**), 1410–1414

[10] K. Sastry, Field assisted sintering and characterization of ultrafine and nanostructured aluminium alloys, PhD thesis, Ku Leuven, 2006, p. 255

[11] K. Vanmeensel, A. Laptev, J. Hennicke, J. Vleugels, O. Van Der Biest, Modelling of the temperature distribution during field assisted sintering, Acta Materialia, 53 (**2005**), 4379–4388

[12] J. Zhang, A. Zavaliangos, Jr. J. Groza, Field activated sintering techniques: a comparison and contrast, Powder Metallurgy Science Technology and Application, 5 (**2003**), 17–21

[13] R. Orrú, R. Licheri, A. Locci, A. Cincotti, G. Cao, Consolidation synthesis of materials by electric current activated/assisted sintering, Materials Science and Engineering R, 63 (**2009**), 127–287